JAAS

ROYAL SOCIETY OF CHEMISTRY

PAPER

View Article Online
View Journal

Cite this: DOI: 10.1039/d4ja00374h

Determination of ultralow iridium concentration in small geological samples using isotope dilution coupled with multiple ion counting inductively coupled plasma mass spectrometry†

Cheng Xu,[ab] Weiqiang Li *[ab] and Shichao An *[ab]

Concentrations of Ir in natural samples can provide useful information for tracing a variety of geological and planetary processes; however, efficient, sensitive, and precise analysis of Ir contents remains challenging, especially for crustal samples that are highly depleted in Ir (*i.e.*, at the pg g^{-1} level). Here we report an analytical method for determining ultralow Ir contents (pg g^{-1} level) in small geological samples (<1 g) by the isotope dilution method (ID) using a multiple ion counting inductively coupled plasma mass spectrometer. An ^{191}Ir-enriched spike was mixed with the sample during sample digestion, followed by the separation and purification of Ir from the rock matrix using AG MP-1 anion exchange resin. Ir isotope ratios were analyzed on a Nu 1700 Sapphire MC-ICP-MS using the multiple ion counting. Our tests indicated that the use of collision cell mass spectrometry with helium and hydrogen as the collision/reaction gases did not offer benefits in removing isobaric interferences for Ir isotope analysis. However, through the combination of chemical purification with conventional wet-plasma mass spectrometry, we attained sufficient accuracy for Ir analysis at ultralow levels. The total procedural blank and detection limit for this method were determined to be 7.6 ± 3.5 pg (2σ, $N = 10$) and 0.35 pg g^{-1}, respectively. To validate the accuracy of this analytical method, a K-Pg boundary reference sample (DINO-1) and six USGS reference materials were analyzed, and the obtained results were consistent with previous studies. Furthermore, we report Ir contents in other 11 international geological reference materials with low Ir abundance, demonstrating the applicability of this method in studying ultralow Ir content samples associated with magmatic processes, supergene processes and impact events.

Received 18th October 2024
Accepted 3rd December 2024

DOI: 10.1039/d4ja00374h

rsc.li/jaas

1 Introduction

Iridium (Ir), a member of the platinum group elements (PGEs), can provide key constraints on a variety of important processes such as planetary differentiation, sulfide-melt interaction, and noble metal mineralization.[1–5] Due to its strong siderophile nature, Ir is primarily concentrated in the core during the early stages of Earth's evolution,[2] subsequently leading to the depletion of Ir in the silicate Earth, especially in the crust (*i.e.*, 22 pg g^{-1} of the upper continental crust[6]). In contrast, meteorites typically contain high levels of Ir.[7] The anomalous iridium enrichment at the Cretaceous–Paleogene (K–Pg) boundary layers has been taken as evidence for a massive meteorite impact event[8,9] that is linked to the extinction of dinosaurs. Concentrations of Ir in geological samples can provide valuable information for many research topics; however, due to the low contents (*i.e.*, sub-ppb level) of Ir in crustal samples, accurate and precise analysis of Ir contents remains highly challenging, consequently restricting more intricate and detailed research studies.

In early studies, neutron activation analysis (NAA) was applied to obtain the Ir contents in geological samples.[8,10,11] For this method, a high flux of neutron radiation is required to achieve sufficient analytical sensitivity, and a substantial cooling period (*i.e.*, one month) is necessary for the radiated samples to ensure safe handling of the radioactive materials.[11] In recent years, inductively coupled plasma mass spectrometry (ICP-MS) has increasingly been applied to analyze the contents of PGEs including Ir.[12–20] However, previously published mass spectrometry methods had limitations in the relatively large sample consumption requirement,[12,14,15,21,22] the relatively high backgrounds or total procedural blanks,[15,16,23] or pre-treatment protocols (fire assay, alkaline fusion, Carius tube digestion, high pressure asher digestion, and co-precipitations)[13,23–25] that are time consuming or technically demanding. Table S1† summarizes the pre-treatment procedures, detection limits,

---

[a] State Key Laboratory for Mineral Deposits Research, School of Earth Sciences and Engineering, Nanjing University, Nanjing, Jiangsu 210023, China. E-mail: liweiqiang@nju.edu.cn; asch@nju.edu.cn

[b] Frontiers Science Center for Critical Earth Material Cycling, Nanjing University, Nanjing, China

† Electronic supplementary information (ESI) available. See DOI: https://doi.org/10.1039/d4ja00374h

procedural backgrounds, and other information of Ir concentration measurements using ICP-MS or NAA methods in the literature. Despite this progress, efficient and sensitive analytical methods for Ir analysis are still in great need for a wide range of applications.

Previous mass spectrometry studies dominantly relied on single-detector mass spectrometers (quadrupole or sector field ICP-MS) that worked in peak-hopping mode, which could limit the sensitivity and precision of Ir analysis. Few studies utilized MC-ICP-MS for the analysis of PGE concentrations. For instance, Jensen *et al.* (2003)[26] used Faraday cups to analyze samples at the ng g^{-1} level, while Chu *et al.* (2015)[19] employed a single electron multiplier in peak-hopping mode to measure samples with low signal intensity. Compared to Faraday cups and the single electron multiplier, the multiple ion counting capability of MC-ICP-MS could offer superior sensitivity and precision for Ir isotope ratio analysis, which would lead to lower detection limits and lower sample consumption for Ir content measurements. To the best of our knowledge, there has been no Ir concentration analysis performed on a multi-collector ICP mass spectrometer (MC-ICP-MS) coupled with a multiple ion counting system in the literature. Furthermore, the latest models of MC-ICP-MS begin to incorporate collision cells (*e.g.*, Nu plasma Sapphire MC-ICP-MS and Neoma MC-ICP-MS), which could reduce the problems of polyatomic interferences during mass spectrometric analysis.[27–29] In this study, we developed a method for ultralow iridium content measurement using isotope dilution mass spectrometry based on multiple ion counting MC-ICP-MS. In addition, we evaluated the potential of collision cell mass spectrometry for Ir analysis. Finally, we reported iridium content data for a wide range of low Ir abundance geological reference materials.

2 Isotope dilution method

The technique of isotope dilution (ID) is widely used for highly accurate and precise determination of element concentrations.[30] In an isotope dilution analysis, a known quantity of a "spike" solution, which contains a non-natural isotope composition, is added to a known quantity of the sample. By measuring the isotope composition of the sample–spike mixture (R_m) using mass spectrometry, the concentration of the target element in the sample can be determined by applying principles of isotope mass balance. The concentration of the sample can be calculated using the equation below:[31]

$$C_\mathrm{sa} = \frac{\mathrm{ab}(193_\mathrm{sp})R_\mathrm{m} - \mathrm{ab}(191_\mathrm{sp})}{\mathrm{ab}(191_\mathrm{sa}) - \mathrm{ab}(193_\mathrm{sa})R_\mathrm{m}} \, \frac{W_\mathrm{sp}C_\mathrm{sp}\mathrm{atwt}(\mathrm{Ir}_\mathrm{sa})}{W_\mathrm{sa}\mathrm{atwt}(\mathrm{Ir}_\mathrm{sp})} \tag{1}$$

where subscripts 'sa', 'sp' and 'm' denote the sample, spike, and sample–spike mixture, respectively. And 'ab', 'atwt', '*W*' and '*C*' represent the abundance, atomic weight, weight and concentration of the spike or sample, respectively. The natural Ir elemental information and isotopic reference values are given by Prohaska *et al.* (2022)[32] and Zhu *et al.* (2017).[33]

The accuracy and repeatability of the calculated sample concentrations heavily rely on the precise determination of both the contents and isotope composition of the spike. Additionally, achieving optimal ratios between the sample and spike is crucial for minimizing the propagation of errors during the measurement process.[34]

The isotope composition of the spike in this study was calibrated by the sample-standard bracketing (SSB) method using mass spectrometry which assumes that the mass bias during analysis of the spike solution is equal to the mean bias of natural standards analyzed before and after the spike. The calibrated isotope composition of the spike $((^{191}\mathrm{Ir}/^{193}\mathrm{Ir})_\mathrm{sp})$ is 40.91 ± 0.02 (2σ, $N = 3$). Once the isotopic composition of the spike was determined, and the masses of the pure iridium standard solution and the spike solution were meticulously measured using a balance scale, the concentration of the spike solution can be accurately determined through reverse isotope dilution. This concentration, specifically, is 32500 ± 500 (2σ, $N = 5$) pg g^{-1} and is diluted 100-fold (*i.e.*, 32.5 ± 5 pg g^{-1}) for subsequent use in the analytical routine.

Following Webster (1959)[35] and Stracke *et al.* (2014),[31] the optimal sample–spike ratio and the error magnification in the isotope dilution method can be determined using eqn (2) and (3). As illustrated in Fig. 1, analytical uncertainty remained small (*i.e.*, error magnification <2) for a fairly wide range of $^{191}\mathrm{Ir}/^{193}\mathrm{Ir}$ ratios of 0.97 to 19.84, corresponding to a spike/sample ratio of 4.00 to 0.04.

$$\left(\frac{^{191}\mathrm{Ir}}{^{193}\mathrm{Ir}}\right)^{\mathrm{opt}}_{\mathrm{mix}} = \sqrt{\left(\frac{^{191}\mathrm{Ir}}{^{193}\mathrm{Ir}}\right)\mathrm{sa}\left(\frac{^{191}\mathrm{Ir}}{^{193}\mathrm{Ir}}\right)\mathrm{sp}} \tag{2}$$

$$F = \left| \frac{\left(\frac{^{191}\mathrm{Ir}}{^{193}\mathrm{Ir}}\right)\mathrm{mix}\left[\left(\frac{^{191}\mathrm{Ir}}{^{193}\mathrm{Ir}}\right)\mathrm{sa} - \left(\frac{^{191}\mathrm{Ir}}{^{193}\mathrm{Ir}}\right)\mathrm{sp}\right]}{\left[\left(\frac{^{191}\mathrm{Ir}}{^{193}\mathrm{Ir}}\right)\mathrm{sa} - \left(\frac{^{191}\mathrm{Ir}}{^{193}\mathrm{Ir}}\right)\mathrm{mix}\right]\left[\left(\frac{^{191}\mathrm{Ir}}{^{193}\mathrm{Ir}}\right)\mathrm{mix} - \left(\frac{^{191}\mathrm{Ir}}{^{193}\mathrm{Ir}}\right)\mathrm{sp}\right]} \right| \tag{3}$$

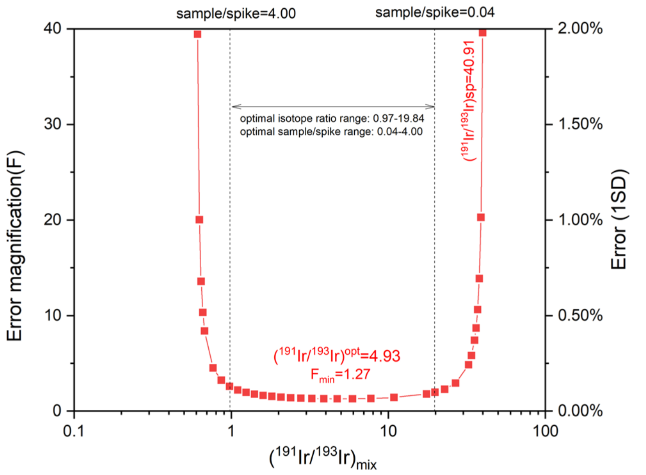

Fig. 1 Plot showing the degree of error magnification in relation to the isotope ratio of the mixture for the Ir spike in this study. The minimum error magnification factor is 1.27, at a $^{191}\mathrm{Ir}$ to $^{193}\mathrm{Ir}$ ratio of 4.93 for the mixture.

3 Experimental

3.1 Materials and reagents

All chemical procedures were performed in an ISO Class 6 clean room with ISO Class 5 fume hoods at the State Key Laboratory for Mineral Deposits Research, Nanjing University. Semiconductor-grade acids (HCl, HNO_3, and HF), Teflon coated hot plates, Teflon beakers and deionized (18.2 MΩ) water were used for all sample preparation and ion-exchange chromatography. Commercially available 100 $\mu g\ g^{-1}$ multi-element stock solutions for column calibrations were supplied by Aladdin (Lot: B2318019). Single-element Ir standard solution used for quantitative analysis was purchased from AccuStandard (Lot: 222025053, 1000 $\mu g\ g^{-1}$). Ir metal ingots enriched in ^{191}Ir were purchased from Isoflex (**http://www.isoflex.com**). The spike was digested and then stored in 10% (v/v) HCl as a stock solution to be diluted for further measurements.

To validate the reliability and accuracy of Ir concentration analysis by isotope dilution using multiple ion counting MC-ICP-MS, we measured the standard sample (DINO-1) which was prepared from the Danish Cretaceous–Paleogene boundary layer,[36] and six USGS reference materials (BHVO-2, BCR-2, BIR-1, Sco-1, MAG-1 and DNC-1). Additionally, we analyzed Ir contents of 11 geological reference materials including mafic intrusive rocks (DTS-2 and W-2), felsic rocks (GSP-2, QLO-1, GSR-1, JG-2, and JR-2), sedimentary rocks (SBC-1, Nod-A-1, and COQ-1) and the metamorphic rock (SDC-1) using the method in this study to supplement the Ir content information of geological reservoirs.

3.2 Sample preparation

Different sample preparation methods have been employed in previous Ir analysis studies: (1) alkali fusion: sample powders are mixed with alkali-flux regents (sodium peroxide and sodium hydroxide), at high temperatures, iridium forms a Na–Ir–O compound with Na_2O_2,[37] which can then be dissolved in acids. (2) Acid digestion in PFA vessels: Yi and Masuda (1996)[18] used this method to dissolve the clay samples of the K-Pg boundary section with a mixture of hydrofluoric acid and perchloric acid, nitric acid and hydrochloric acid in a Teflon beaker. (3) High-pressure ashing (HPA-S): sample dissolution is performed under the conditions of >100 bar and 300 °C.[23] (4) Acid digestion in Carius tubes: this method involves the use of concentrated HCl and HNO_3 in sealed quartz tubes at approximately 240 °C for at least one day to effectively digest iridium-bearing samples.[25] (5) Acid digestion in a high pressure bomb: a pressure of ∼1200 psi with mixed concentrated acid at about 150–200 °C for 1–2 days is used to digest iridium-bearing samples.[38,39] (6) Nickel fire assay: NiS is used as a collector to preconcentrate PGEs.[16,21,40] The drawback of this method is that it requires large amounts of samples and salts, which leads to an elevated blank level and potential contamination.

The "acid digestion in PFA vessels" method was selected in our study, considering its efficiency and the potential to minimize other sources of contamination. Approximately 50 to 1000 mg of rock powder were digested in a Teflon beaker with 8 ml of a 1 : 1 mixture of HNO_3 : HF on a hotplate at 130 °C for over 24 hours after mixing them with the spike solution within the optimal dilution ratio range ($^{191}/^{193}$Ir range: 0.97–19.84; the concentration of Ir in the sample is estimated by considering its lithology and reference data from previous studies). Then the solution was evaporated to dryness at 120 °C and redissolved in 8 ml of aqua regia for more than one day and then dried. This step can effectively remove fluorides and achieve isotope equilibrium. Yi and Masuda (1996),[41] in their comparison of various methods for attaining Ir isotope equilibrium, found that heating on a 150 °C hotplate for 10 minutes achieved an isotope ratio that was remarkably close to the theoretical ratio. After that, the sample was dissolved in 8 ml of concentrated HCl and refluxed at 130 °C for one day and then dried. Afterwards, the sample was redissolved in 0.5 M HCl and centrifuged prior to ion exchange chromatography separation.

3.3 Column chemistry

In chloride media, iridium primarily exists in the forms of Ir(III)Cl_6^{3-} and Ir(IV)Cl_6^{2-}.[42] Consequently, Ir can be effectively separated from most matrix elements, including K, Mg, Na, Al, *etc.* during anion exchange chromatography. Here, 2 mL of anion exchange resin (Bio-Rad AG MP-1, 100–200 mesh) was loaded into a RISKEM® plastic column (No. AC-142-TK) with an internal diameter of 7 mm. Following the loading of the resin, it was pre-cleaned sequentially with Milli-Q water, 4.5 M HNO_3, and 7 M HCl. Subsequently, it was conditioned with 0.5 M HCl. After the sample was loaded, the matrix elements were eluted from the column using 0.5 M HCl. Then Ir was recovered using 15 mL of 7 M HCl (Table 1). The purified Ir fractions were then dried at 100 °C and dissolved in 2% HNO_3.

3.4 Mass spectrometry

All Ir isotope analyses were performed on a Nu 1700 Sapphire MC-ICP-MS at the State Key Laboratory for Mineral Deposits Research and Frontiers Science Center for Critical Earth Material Cycling, Nanjing University. All the parts for solution introduction, such as the nebulizer, spray chamber, torch, and cones, were carefully cleaned before usage. The sample solutions were introduced into the Ar plasma with a 70 µL per min PFA nebulizer. The signals for ^{191}Ir and ^{193}Ir were measured utilizing dual ion counters, specifically discrete dynode

Table 1 Chromatographic procedures for the separation of Ir using AG MP-1 resin

Step	Eluent	Volume/mL
2 mL AG MP-1 resin (100–200 mesh)		
Cleaning	H_2O	5
—	4.5 M HNO_3	5
—	H_2O	5
—	7 M HCl	5
—	H_2O	5
Conditioning	0.5 M HCl	5
Sample loading	0.5 M HCl	4
Matrix elution	0.5 M HCl	12
Ir collection	7 M HCl	15

Table 2 Instrumental operation parameters for Ir isotope measurement using a Nu 1700 Sapphire MC-ICP-MS

Parameters	Value
RF power	1300 W
Auxiliary gas flow rate	1.0 L min^{-1}
Sample gas flow rate	0.9 L min^{-1}
Plasma cooling gas flow rate	13.0 L min^{-1}
Measurement mode	Static
Interface cones	Standard Ni cones
Acceleration voltage	−6000 V
Detectors	Discrete dynode multipliers (count limit: 2 million cps)
Operational voltages for ion counters	2000–2500 V
Sample measurement time	40 × 3 s integrations
Instrument resolution	Low
Nebulizer	MicroFlow PFA-70 μL min^{-1}
Sample introduction system	Wet plasma mode with glass cyclonic spray chamber
Solution concentration	pg per g level
Cup configuration	IC2 IC3 ^{193}Ir ^{191}Ir

multipliers, each with a count limit of 2 million counts per second (cps). The ion counters were tuned following the manual from the manufacturer before performing ion counting. The data acquisition sequence consists of 40 seconds of sample uptake time and 40 cycles with an integration time of 3 seconds. The instrument was operated with a standard 1300 W forward RF power at low mass resolution (resolving power is 400). The sensitivity of the instrument was approximately 1.6 million cps per ng g^{-1}. Between two measurements, a two-minute wash with 2% HNO_3 was conducted to ensure proper cleaning. Background counts of 2% HNO_3 solution and air are routinely lower than 50 and 20 cps, respectively. The detailed instrument settings and operational parameters for data acquisition are summarized in Table 2.

The instrumental mass bias in Ir isotope ratio measurements was corrected utilizing the SSB method, identical to the approach applied for calibrating the isotope ratio of the spike.

4 Results and discussion

4.1 Separation and purification processes of iridium using ion exchange chromatography

The presence of significant amounts of impurity elements in the solution can introduce matrix effects and interferences during ICP mass spectrometry, compromising the analytical accuracy. Essential separation and purification procedures are needed to ensure the accuracy and reliability of subsequent analysis. Both cation exchange chromatography[24,38] and anion exchange chromatography[18,19,23,43] have been applied to PGE analyses of geological materials.[42,44,45] One disadvantage with cation separations is the relatively large quantities of resin and acids to retain the large amounts of the cation matrix on the column. Therefore, in this study, the AG MP-1 anion exchange resin was used, and the matrix was eluted with low-concentration hydrochloric acid followed by recovery of Ir solutions using the high-concentration hydrochloric acid eluent.

The elution curves of various elements using the AG MP-1 resin column procedures are shown in Fig. 2. Most matrix elements were efficiently eluted from the column using 0.5 M HCl. Subsequently, iridium was recovered by elution with 7 M HCl. Analysis of the elution curve reveals that approximately 14.5% ± 5.6% (2σ, $N = 3$) of Ir was prematurely eluted in 0.5 M HCl media, while the recovery of iridium in 7 M HCl was 84.6 ± 8.5% (2σ, $N = 3$). The results are in alignment with those reported by Yi and Masuda (1996),[18] who investigated the retention of Ir in hydrochloric acid media at different concentrations. Their study indicated that approximately 14% of Ir remained unadsorbed onto anion resin in a 0.5 M HCl medium. It should be noted that the isotope dilution method is inherently immune to incomplete recovery during the separation and purification processes,[30] thus the non-quantitative recovery of Ir during chemistry does not affect the Ir concentration analysis as long as the Ir spike and samples are equilibrated during sample dissolution.

4.2 Performance of multiple ion counting Ir isotope ratio measurements

As discussed in the preceding section, the precision of concentration measurements by isotope dilution (ID) is heavily

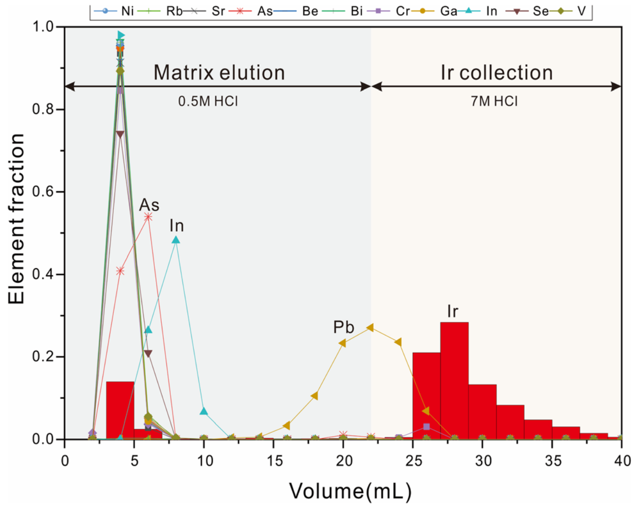

Fig. 2 Elution curves for iridium and other elements in the matrix of the synthetic solution using 2 ml of AG MP-1 resin.

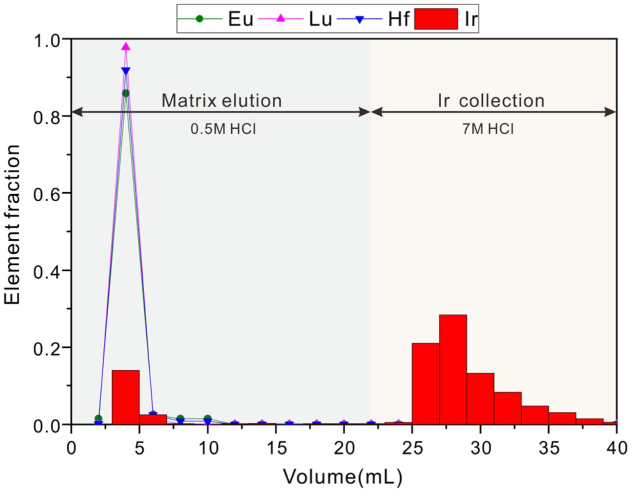

Fig. 3 Elution curves for the separation of Ir from the interference elements (Lu, Hf, and Eu).

dependent on the accuracy of the determined isotope ratios, including those of the spike and the spike-sample mixtures. The precision of the Ir isotopes must be assessed before conducting the analysis, particularly when the isotopes are collected and measured using ion counters, as is the case in this study. To ensure the basic functionality of the ion counters, tests were carried out to evaluate their sensitivity, linear dynamic range, and the accuracy of isotope ratio measurements through multiple ion counting. In light of this, a series of Ir solutions with concentrations ranging from 0.87 to 1057 pg g^{-1}, without the addition of spike, were prepared gravimetrically. Subsequently, the isotope intensities and isotope ratios were measured for these solutions. The results are presented in Table S2† and Fig. 4. The data exhibit an excellent linear relationship between isotope counts and Ir concentrations, which attests to the wide linear dynamic range of the ion counters. It is important to note that the count limit for each ion counter in this instrument is 2 million cps, and the count rate for a 1057 pg g^{-1} concentration is close to 1.5 million cps. This suggests that the response of the ion counter is likely linear across the entire measurement range of the ion counters. The uncertainties of the isotope ratios decrease with increasing Ir concentrations when below 86 pg g^{-1}, but do not further improve at concentrations above 86 pg g^{-1}, as shown in Fig. 4. To further ascertain the efficacy of the multiple ion counting technique, an additional series of pure Ir solutions, spiked with known

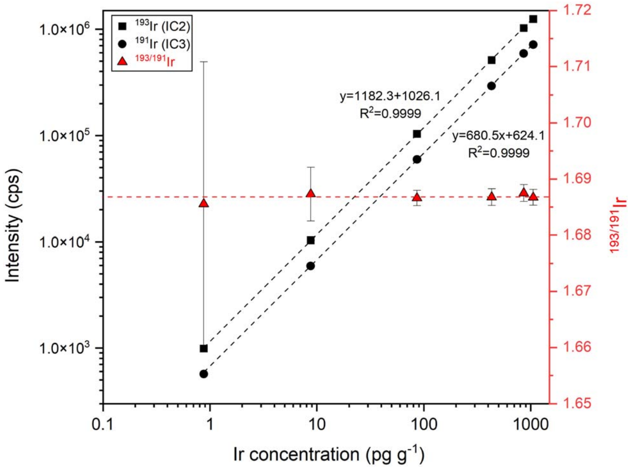

Fig. 4 The performance of multiple ion counting for test Ir (isotopically normal) solutions. The black symbols represent the intensities of ^{193}Ir and ^{191}Ir at various Ir concentrations, with the black dashed line indicating the linear fitting trend. The red symbols show the isotope ratio at different Ir concentrations, while the red dashed line indicates the natural Ir isotope ratio ($^{193/191}$Ir = 1.6866 (ref. 33)). For raw data, see Table S2.†

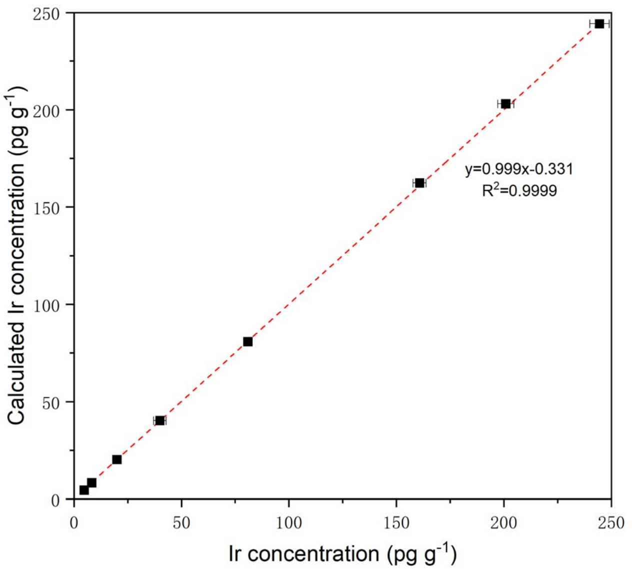

Fig. 5 Calculated Ir concentrations *versus* the actual Ir concentrations at the optimum isotope ratio, spanning from low to high intensities. For raw data, see Table S3.†

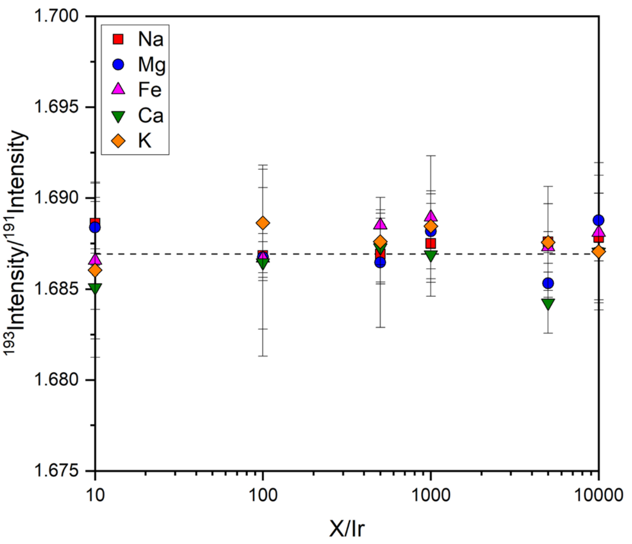

Fig. 6 Effects of major matrix elements on Ir isotope measurements in a 1 ppb Ir solution. The matrix elements (X) include Ca, Mg, Na, K, and Fe. For raw data, see Table S4.†

concentrations at the optimal isotope ratios, were measured for their isotope ratios, and the concentrations were subsequently calculated. The results are displayed in Table S3† and Fig. 5. The close concordance between the actual and calculated concentrations demonstrates the high degree of accuracy and dependability of this method when employing the multiple ion counting system.

4.3 Isobaric interferences and matrix effects

During isotope analysis using the MC-ICP-MS, the sample solution is introduced into the ICP and ionized efficiently. However, certain elements or their combinations with plasma gas, solvents, and acids can introduce interferences in the analysis of target isotopes, including doubly charged and polyatomic interferences.[27] For iridium isotope analysis, $^{175}Lu^{16}O^+$, $^{151}Eu^{40}Ar^+$, and $^{190}Os^1H^+$ could interfere with ^{191}Ir, and $^{177}Hf^{16}O$, $^{153}Eu^{40}Ar^+$, $^{192}Pt^1H^+$, and $^{193}Os^1H^+$ could interfere with ^{193}Ir.[46] Additionally, the existence of major elements (Mg, Fe, Ca, K, Na, *etc.*) in the solution can also affect isotope ratio analysis by matrix effects.[47,48] Although the majority of matrix elements are removed through the ion exchange process, their residuals could still be significant compared to the sub-ppb level of Ir.

To evaluate the impact of matrix effects and the isobaric interferences on Ir isotope analyses, we doped a series of major matrix elements and Lu, Hf, Eu, Os, and Pt into pure Ir solutions at the mass ratios of [X]/[Ir] (10^3 pg g^{-1}/10^3 pg g^{-1}) varying from 0.01 to 10 000. The results show that the Ir isotope ratio analysis is unaffected by matrix effects of major elements (Fig. 6 and Table S4†) but could be significantly influenced by isobaric interferences (Fig. 7 and Table S5†). When [X]/[Ir] is larger than

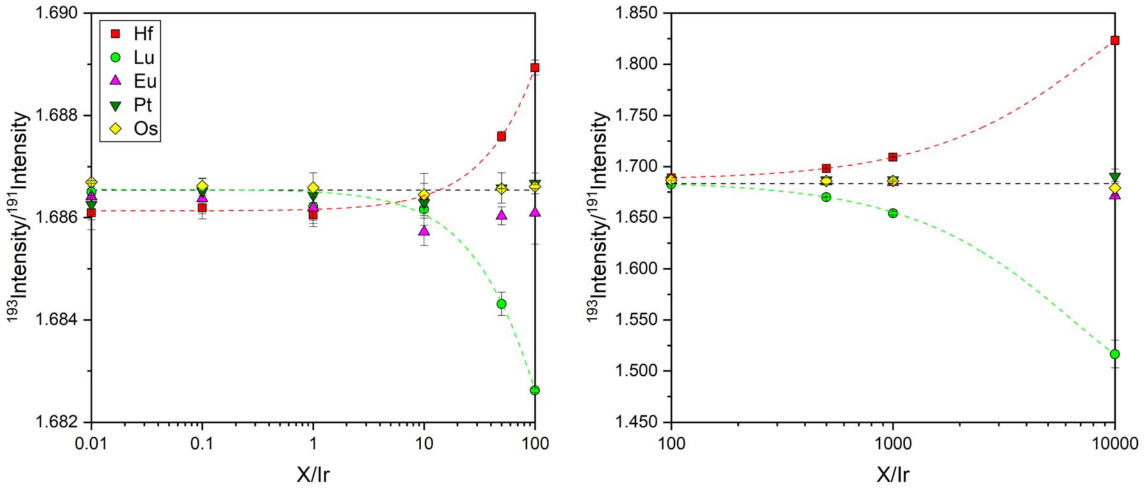

Fig. 7 Doping experiments for Hf, Lu, Eu, Pt and Os to test the effect of their interferences on Ir isotope measurements. For raw data, see Table S5.†

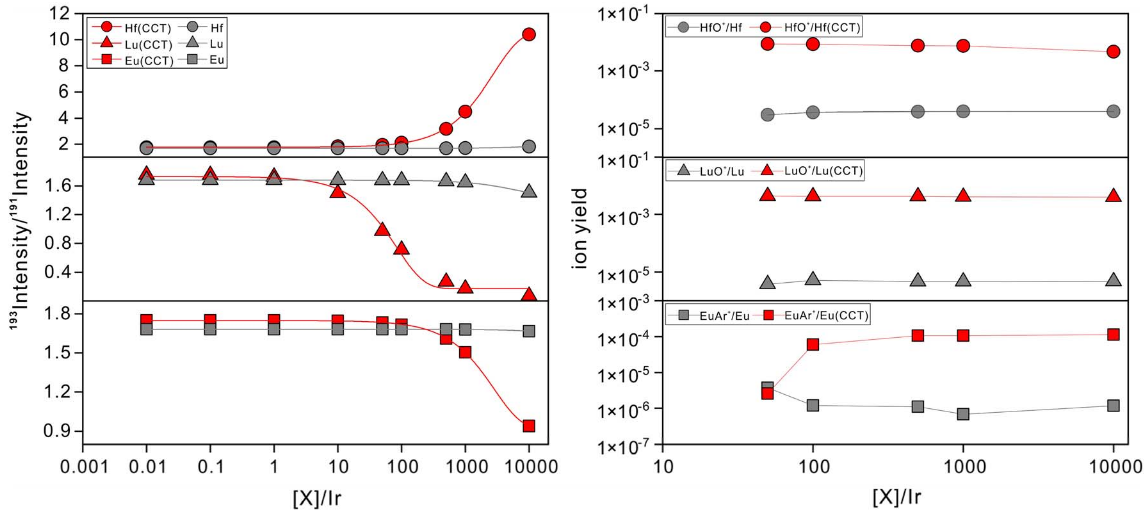

Fig. 8 Isotope ratio and interferent ion yield of using the collision cell (CCT) (H_2 and He as reaction and collision gases, and flow rates are 5 and 3 ml min^{-1}, respectively.) *versus* [X]/[Ir]. The ion yield is equal to the signal of the oxide or argonide divided by the signal of the interfering element itself such as HfO/Hf. For raw data, see Tables S6 and S7.†

100, Hf and Lu can cause non-negligible interference to Ir isotope measurements. Therefore, it is necessary to reduce the content of these elements or minimize the ion yield of their isotopic analogues.

Generally, when performing isotope analysis using ICP-MS, there are several methods to eliminate or reduce isobaric interferences from oxides, argonides and hydrides, including (1) pre-analysis chemical separation and purification, (2) post-analysis corrections of interferences, and (3) changing instrument settings.[46]

We first evaluated the effect of ion exchange chromatography. As shown in Fig. 3, Ir can be effectively separated from these three interference elements (Eu, Lu, and Hf). The elution efficiencies of Eu, Lu, and Hf using 0.5 M HCl to remove matrix elements were found to be efficient, with removal ratios of 99.4 ± 0.1%, 99.3 ± 0.3% and 99.6 ± 0.2%, (2σ, $N = 4$), respectively. This means that <0.5% of these three interference elements for Ir may remain after the column chemistry. Felsic rocks generally have the lowest Ir contents and highest rare earth elements, thus would have the worst interference problem for Ir. Taking the granite rock standard (GSR-1) as an example, it contains 4 pg per g (ppt) Ir, 6.3 μg per g (ppm) Hf, 1.15 μg per g Lu, and 0.85 μg per g Eu. Assuming a matrix removal rate of 99.5%, after the ion-exchange chromatography in our study, the Hf/Ir, Lu/Ir and Eu/Ir ratios were lowered to 6300, 2012 and 1275, respectively. Based on the doping experiments shown in Fig. 7, the interference by Hf and Lu would collectively deviate the Ir ratio value by about 5%. However, for other more mafic samples that would have lower REE contents but higher Ir, the interference issue by Hf, Lu, and Eu would be significantly less profound. Hence, the uncertainty of isotope ratio analysis of Ir for column processed geological samples is expected to be better than 5% (RSD, relative standard deviation). The error propagated to the final calculated concentrations will be at a level less than 6% (for more details, see the discussion in Section 4.4). The interference issue could be further reduced by repeating the column procedure, however, this would introduce a higher total procedural blank and lower sample processing efficiency. An uncertainty level of 6% RSD in Ir concentration would be sufficient for the majority of geological applications because the Ir concentration variability among different geological samples can be much greater (*e.g.*, sub-ppb level to ppm level).

In recent years, an ICP-MS equipped with collision/reaction cells has become increasingly accessible, enabling the reduction or elimination of polyatomic interferences in ICP analysis.[27,49] In this study, the Nu 1700 Sapphire MC-ICP-MS was tested in collision cell mode using He + H_2 as the collision/reaction gas for Ir isotope analysis. However, the results (Fig. 8) indicated increased polyatomic interference compared to conventional ICP-MS. This may be attributed to the low mass of He and H_2, which is insufficient to thermalize incoming ions and reduce interferences.

Based on the tests shown above, purification by one-stage ion exchange chromatography combined with conventional wet-plasma mass spectrometry has demonstrated the capability to deliver sufficient accuracy for Ir isotope analyses. We note that the full potential of the collision cell in Ir isotope analysis is yet to be further explored, as we only tested with He and H_2 gases, which have proven effectiveness for K, Ca, and Fe isotope analyses,[27–29,49] but likely not with heavier ions such as HfO^+ and LuO^+. It is possible that heavier collision gases (*e.g.*, Ar and Xe) and other reactive gases (*e.g.*, NH_3) will be effective in removing polyatomic inferences for Ir isotopes, which remains to be explored in future work.

4.4 Estimated uncertainties for analysis of Ir concentrations

Reasonably evaluating uncertainties constitutes a crucial step in isotope dilution analysis. The accuracy and precision of the

Table 3 Estimated and propagated uncertainties of parameters and terms in eqn (1)

Parameter in eqn (1)	Absolute value	Relative uncertainty	Absolute uncertainty
W_{sa} (g)	1.00000	0.1%	0.001
W_{sp} (g)	0.038	0.1%	0.000038
C_{sp} (pg g^{-1})	325	1.5%	5
$^{191/193}Ir_{sp}$	40.91	0.05%	0.02
ab(191_{sp})	0.976	0.07%	0.00067
ab(191_{sa})	0.373	0.05%	0.0002
atwt(Ir_{sp})	191.002	0.1%	0.191
atwt(Ir_{sa})	192.217	0.001%	0.002
R_m	4.93	5%	0.2465
Term in eqn (1)	Absolute value	Propagated relative uncertainty	Propagated absolute uncertainty
W_{sp}/W_{sa}	0.039	0.14%	0.00005
Conc$_{sp}$ (pg g^{-1})	325	1.50%	5
atwt(Ir_{sa})/atwt(Ir_{sp})	1.006	0.10%	0.001
ab(193_{sp})R_m − ab(191_{sp})/ab(191_{sa}) − ab(193_{sa})R_m	0.310	5.72%	0.018
Conc$_{sa}$ (pg g^{-1})	3.96	5.91%	0.23

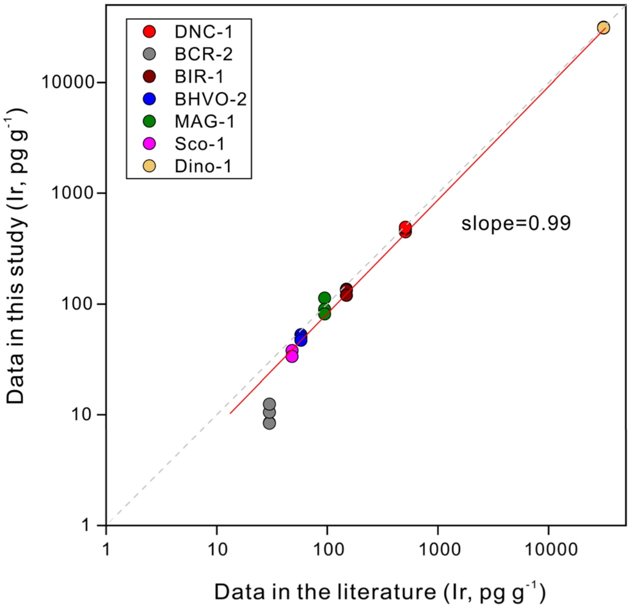

Fig. 9 Comparison of Ir contents in reference materials between this study and the literature.[36,50]

sample concentrations determined by isotope dilution rely not only on instrumental measurement errors but also on the uncertainties associated with the parameters in eqn (1). These include errors in weighing, spike calibration, and so on. Table 3 shows the parameters utilized in eqn (1), along with the estimated uncertainties for the analysis of Ir isotope dilution using GSR-1 as a case study. Additionally, it presents the propagated uncertainties for each term in eqn (1).

The uncertainty of weight is conservatively estimated to be 1 mg (0.1%). Moreover, based on the results of spike calibration, the uncertainties of conc_{sp} and $^{191/193}\text{Ir}_{\text{sp}}$ are determined directly. Then, the uncertainties of $\text{ab}(^{191}\text{Ir}_{\text{sp}})$ and $\text{atwt}(\text{Ir}_{\text{sp}})$ are calculated. The values of "$\text{ab}(191_{\text{sa}})$" and "$\text{atwt}(\text{Ir}_{\text{sa}})$" were adopted from IUPAC-recommended natural abundance and atomic weights of Ir. Finally, the 5% uncertainty of R_{m} is estimated based on the current chemical process, taking the felsic rock (GSR-1) as an example, which is rich in Hf and Lu, and depleted in Ir. For other rock types, this uncertainty should be much lower. After propagating all uncertainties of the parameters in eqn (1), we could get the theoretical relative error at a level less than 5.9% in this work.

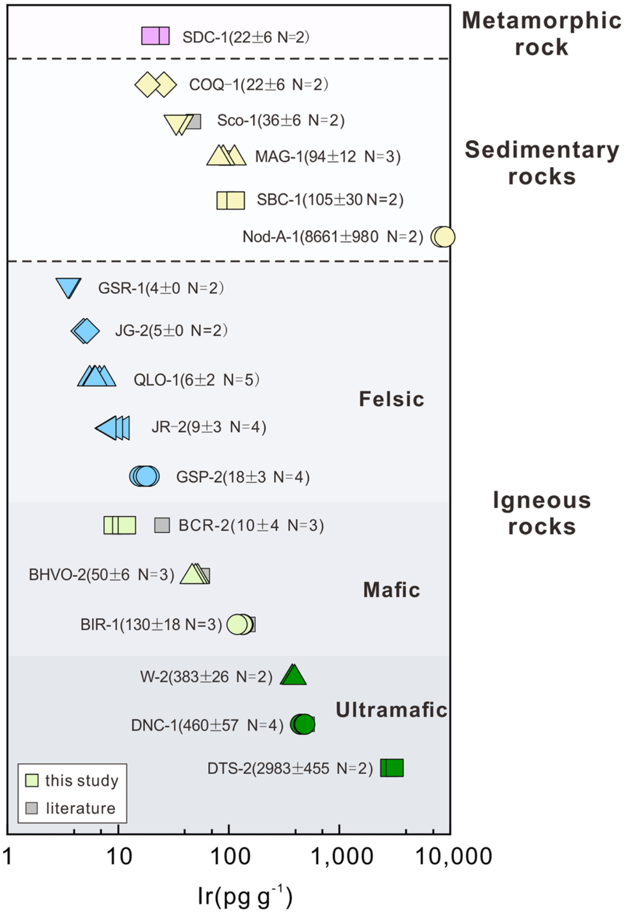

Fig. 10 Ir contents of geological reference materials measured in this study compared with the literature.[50]

4.5 Procedural blank and detection limits

The total procedural blank was prepared by following the same method as that used for a natural sample. Specifically, 100 µl of spike was added to a clean Teflon beaker, and a digestion process was carried out, which involved concentrated nitric acid, hydrofluoric acid, followed by aqua regia, and then concentrated hydrochloric acid. Subsequently, the solution was converted to a 0.5 M HCl medium for the ion exchange chromatography step. Ten total procedural blanks were measured, resulting in an average blank level of 7.6 ± 3.5 pg (2σ, $N = 10$) for Ir across all analytical procedures.

Table 4 Ir contents (pg g^{-1}) from this work *vs.* reference values

Sample	DINO-1	BHVO-2	BCR-2	BIR-1	Sco-1	MAG-1	DNC-1
Average ± 2SD	31037 ± 293	50 ± 6	10 ± 4	130 ± 18	36 ± 6	94 ± 12	460 ± 57
N	7	3	4	3	4	2	3
Alvarez *et al.* (1982)[36]	31500 ± 600	—	—	—	—	—	—
Meisel and Moser (2004)[50]	—	58 ± 30	30 ± 7	149 ± 63	48 ± 21	95 ($N = 1$)	510 ($N = 1$)
Li *et al.* (2014)[13]	—	65 ± 12	—	—	—	—	—
Ishikawa *et al.* (2014)[51]	—	—	—	143 ± 17	22 ± 12	—	—
Chu *et al.* (2015)[19]	—	80 ± 10	6 ± 0	136 ± 10	—	—	431 ± 39

Table 5 Concentration results of 11 reference materials from this study

Sample	DTS-2	W-2	GSP-2	QLO-1	GSR-1	JG-2	JR-2	SBC-1	Nod-A-1	SDC-1	COQ-1
Average ± 2SD	2983 ± 455	383 ± 26	18 ± 3	6 ± 2	4 ± 0	5 ± 0	9 ± 3	105 ± 30	8661 ± 980	22 ± 6	22 ± 6
N	2	2	4	5	2	2	4	2	2	2	2

The detection limit was calculated as three times the standard deviation of 10 individual procedural blank values, which is 0.35 pg g^{-1} for Ir (for a 1 g sample, a final volume of 15 ml). The procedural blank and detection limits of this method are sufficient to meet the requirements for the analysis of samples with ultralow Ir contents.

4.6 Reproducibility

To validate the precision and accuracy of this method, a certified Ir-standard material (DINO-1) that was prepared from the Danish Cretaceous–Paleogene boundary layer[36] was analyzed independently in different sessions 7 times. Six USGS reference materials (BHVO-2, BCR-2, BIR-1, Sco-1, MAG-1 and DNC-1) were also analyzed and compared to previous studies.[13,19,50,51] As shown in Fig. 9 and Table 4, the Ir concentrations measured in this study are consistent with literature values. Additionally, the relative standard deviations of multiple repeat analyses are smaller in this study, supporting the accuracy and reproducibility of our method. Additionally, this study measured Ir concentrations in 11 new international geological reference materials with low Ir abundance, including mafic rocks (DTS-2 and W-2), felsic rocks (GSP-2, QLO-1, GSR-1, JG-2, and JR-2), sedimentary rocks (SBC-1, Nod-A-1, and COQ-1), and a metamorphic rock (SDC-1). The results, presented in Fig. 10, Tables 5 and S8,† reveal a highly heterogeneous distribution of Ir in the Earth's crust. Notably, despite high Ir concentrations in certain samples, such as DTS-2 and Nod-A-1, approximately 1 gram of the dissolved sample is required to achieve reliable reproducibility. This requirement may be attributed to the nugget effect associated with platinum-group elements (PGEs). Based on the above results, the method developed in this study can be effectively applied to measure Ir concentrations in various geological samples, both low and high, providing key constraints on the geochemical behavior of Ir in magmatic-hydrothermal processes, sedimentary processes, as well as impact events.

5 Conclusions

In this study, we developed a method for determining ultralow levels (10^{-12} g g^{-1}, ppt) of iridium in small geological samples using isotope dilution coupled with multiple ion counting MC-ICP-MS. The acid digestion method was chosen due to its dissolution efficiency and low blanks. The effects of matrix and isobaric interferences were systematically evaluated. The results show that matrix effects from major rock forming cations (*e.g.*, Mg, Ca, and K) are negligible but isobaric interferences (LuO^+ and HfO^+) could significantly affect the Ir isotope ratio measurements. Anion exchange chromatography could remove the interfering elements to a negligible degree. We estimated the uncertainties and performed error propagation calculations, yielding a theoretical error level of <6% (RSD). The procedural blank and detection limit for Ir are 7.6 pg and 0.35 pg g^{-1}, respectively. The reliability and accuracy were verified by measuring the K-Pg boundary reference material (DINO-1) and USGS reference materials (BHVO-2, BCR-2, BIR-1, DNC-1, MAG-1, and SCo-1), with results that match well with previous studies. Additionally, Ir concentrations of 11 low abundance reference materials were reported in this study, suggesting that this method could be applied to analyze samples with low Ir abundance and provide key constraints for a variety of problems.

Data availability

The data underlying this article are available in the article and in its online ESI.†

Author contributions

Cheng Xu: data curation, formal analysis, investigation, writing – original draft, review & editing. Weiqiang Li: conceptualization, methodology, resources, writing – review & editing, supervision, project administration, funding acquisition. Shichao An: methodology, investigation, supervision, writing – review & editing.

Conflicts of interest

There are no conflicts of interest to declare.

Acknowledgements

This study was supported by the National Natural Science Foundation of China (Grant No. 42425301 to WL) and the Fundamental Research Funds for the Central Universities (Grant No. 020614380203) to WL. We thank Birger Schmitz for providing the DINO-1 Ir reference standard material and inspiring us to develop this analytical method.

References

1 S. J. Barnes and C. P. Picard, *Geochim. Cosmochim. Acta*, 1993, **57**, 79–87.

2 X. Song, R. Hu and L. Chen, *Geosci. Front.*, 2009, **16**, 19.

3 D. Tang, K. Qin, B. Liu, H. Sun and J. Li, *Acta Petrol. Sin.*, 2008, **24**, 569–588.

4 R. J. Walker, *Geochemistry*, 2009, **69**, 101–125.

5 B. Peucker-Ehrenbrink, G. Ravizza and G. Winckler, *Elements*, 2016, **12**, 191–196.
6 B. Peucker-Ehrenbrink and B. M. Jahn, *Geochem., Geophys., Geosyst.*, 2001, **2**, 2001GC000172.
7 E. Anders and N. Grevesse, *Geochim. Cosmochim. Acta*, 1989, **53**, 197–214.
8 L. W. Alvarez, W. Alvarez, F. Asaro and H. V. Michel, *Science*, 1980, **208**, 1095–1108.
9 R. Ganapathy, *Science*, 1980, **209**, 921–923.
10 C. E. Dunn, G. E. M. Hall and E. Hoffman, *J. Geochem. Explor.*, 1989, **32**, 211–222.
11 M. Ebihara, N. Shirai, J. Kuwayama and Y. Toh, *Nucl. Eng. Technol.*, 2022, **54**, 423–428.
12 W. Ni, X. Mao and H. Zhang, *Anal. Lett.*, 2019, **52**, 1699–1710.
13 J. Li, X.-Y. Jiang, J.-F. Xu, L.-F. Zhong, X.-C. Wang, G.-Q. Wang and P.-P. Zhao, *Geostand. Geoanal. Res.*, 2014, **38**, 37–50.
14 J. Amossé, *Geostand. Newsl.*, 2007, **22**, 93–102.
15 L. Qi, M. F. Zhou and C. Y. Wang, *J. Anal. At. Spectrom.*, 2004, **19**, 1335–1339.
16 S. E. Jackson, B. J. Fryer, W. Gosse, D. C. Healey, H. P. Longerich and D. F. Strong, *Chem. Geol.*, 1990, **83**, 119–132.
17 D. Colodner, E. A. Boyle and J. M. Edmond, *Anal. Chem.*, 1993, **65**, 1419–1425.
18 Y. V. Yi and A. Masuda, *Anal. Chem.*, 1996, **68**, 1444–1450.
19 Z. Chu, Y. Yan, Z. Chen, J. Guo, Y. Yang, C. Li and Y. Zhang, *Geostand. Geoanal. Res.*, 2015, **39**, 151–169.
20 B. Peucker-Ehrenbrink, C. A. Waters, M. D. Kurz and P. F. Hoffman, *Earth Planet. Sci. Lett.*, 2016, **437**, 76–88.
21 K. Oguri, G. Shimoda and Y. Tatsumi, *Chem. Geol.*, 1999, **157**, 189–197.
22 X. Jin and H. Zhu, *J. Anal. At. Spectrom.*, 2000, **15**, 747–751.
23 T. Meisel, J. Moser, N. Fellner, W. Wegscheider and R. Schoenberg, *Analyst*, 2001, **126**, 322–328.
24 O. A. Tyutyunnik, S. N. Nabiullina, M. O. Anosova and I. V. Kubrakova, *J. Anal. Chem.*, 2020, **75**, 769–777.
25 W. Pretorius, D. Chipley, K. Kyser and H. Helmstaedt, *J. Anal. At. Spectrom.*, 2003, **18**, 302–309.
26 K. K. Jensen, J. Baker, T. Waight, R. Frei and D. W. Peate, *Geostand. Newsl.*, 2003, **27**, 59–66.
27 W. Li, B. L. Beard and S. Li, *J. Anal. At. Spectrom.*, 2016, **31**, 1023–1029.
28 J. Wang, D.-M. Tang, B.-X. Su, Q.-H. Yuan, W.-J. Li, B.-Y. Gao, K.-Y. Chen, Z.-A. Bao and Y. Zhao, *J. Anal. At. Spectrom.*, 2022, **37**, 1869–1875.
29 W. Dai, F. Moynier, M. Paquet, J. Moureau, B. Debret, J. Siebert, Y. Gerard and Y. Zhao, *Chem. Geol.*, 2022, **590**, 120688.
30 P. Bedson, *Guidelines for Achieving High Accuracy in Isotope Dilution Mass Spectrometry (IDMS)*, Royal Society of Chemistry, 2002.
31 A. Stracke, E. E. Scherer and B. C. Reynolds, *Treatise on Geochemistry*, 2nd edn, 2014, vol. 15, pp. 71–86.
32 T. Prohaska, J. Irrgeher, J. Benefield, J. K. Böhlke, L. A. Chesson, T. B. Coplen, T. Ding, P. J. H. Dunn, M. Gröning, N. E. Holden, H. A. J. Meijer, H. Moossen, A. Possolo, Y. Takahashi, J. Vogl, T. Walczyk, J. Wang, M. E. Wieser, S. Yoneda, X.-K. Zhu and J. Meija, *Pure Appl. Chem.*, 2022, **94**, 573–600.
33 Z. Zhu, J. Meija, A. Zheng, Z. Mester and L. Yang, *Anal. Chem.*, 2017, **89**, 9375–9382.
34 D. Tan, W. Xu, Z. Zhu, S. Li, G. Wu and H. Qin, *Acta Geochim.*, 2020, **39**, 192–202.
35 R. K. Webster, in *Advances in Mass Spectrometry*, ed. J. D. Waldron, Pergamon, 1959, pp. 103–119, DOI: 10.1016/B978-0-08-009210-2.50013-4.
36 W. Alvarez, F. Asaro, H. V. Michel and L. W. Alvarez, *Science*, 1982, **216**, 886–888.
37 J. Lee and Y. Kim, *Mater. Trans.*, 2011, **52**, 2067–2070.
38 J. C. Ely, C. R. Neal, J. A. O'Neill and J. C. Jain, *Chem. Geol.*, 1999, **157**, 219–234.
39 L. Qi, J. Gao, X. Huang, J. Hu, M.-F. Zhou and H. Zhong, *J. Anal. At. Spectrom.*, 2011, **26**, 1900–1904.
40 G. Ravizza and D. Pyle, *Chem. Geol.*, 1997, **141**, 251–268.
41 Y. V. Yi and A. Masuda, *Anal. Sci.*, 1996, **12**, 7–12.
42 D. A. Fine, *J. Inorg. Nucl. Chem.*, 1970, **32**, 2731–2742.
43 A. Makishima, M. Nakanishi and E. Nakamura, *Anal. Chem.*, 2001, **73**, 5240–5246.
44 J.-c. Lee, Kurniawan, H.-J. Hong, K. W. Chung and S. Kim, *Sep. Purif. Technol.*, 2020, **246**, 116896.
45 D. G. Pearson and S. J. Woodland, *Chem. Geol.*, 2000, **165**, 87–107.
46 O. Grebneva and I. Kubrakova, *J. Anal. Chem.*, 2020, **75**, 275–285.
47 J.-X. She, W. Li, S. An and Y. Cai, *J. Anal. At. Spectrom.*, 2023, **38**, 142–155.
48 S. An, X. Luo and W. Li, *Rapid Commun. Mass Spectrom.*, 2022, **36**, e9289.
49 S. An, J. Chen, S. Boschi and W. Li, *Anal. Chem.*, 2023, **95**, 2140–2145.
50 T. Meisel and J. Moser, *Geostand. Geoanal. Res.*, 2004, **28**, 233–250.
51 A. Ishikawa, R. Senda, K. Suzuki, C. W. Dale and T. Meisel, *Chem. Geol.*, 2014, **384**, 27–46.